

A Method for Extracting Aerodynamic Coefficients from Free-Flight Data

GARY T. CHAPMAN* AND DONN B. KIRK†
NASA Ames Research Center, Moffett Field, Calif.

Methods now used to obtain aerodynamic coefficients from free-flight data introduce assumptions and limitations into the equations of motion (e.g., linear aerodynamics, small amplitudes of oscillation, constant roll rate, etc.) so that closed-form solutions can be obtained. Experimental free-flight data are then "fit" by adjusting coefficients and initial conditions in these expressions. A method described herein eliminates the need for closed-form solutions by employing numerical solutions to the equations of motion. This makes possible a far more general treatment. A least-squares technique employing differential corrections must be used; for this, partial derivatives of each dependent variable with respect to each unknown coefficient, including all initial conditions, must be known accurately at every data station. Application of the method of parametric differentiation yields the required accuracy in these partial derivatives and rapid convergence of the solution is usually obtained. Four cases are presented to illustrate specific points: 1) linear aerodynamics, duplication of existing methods; 2) nonlinear aerodynamics, simultaneous analysis of four ballistic-range flights of models of the Gemini capsule; 3) varying freestream density along a trajectory; and 4) large amplitude (to 40° resultant angle of attack) rolling motion of a trimmed Apollo Command Capsule model.

Introduction

MOST of the methods presently in use for obtaining aerodynamic coefficients from an observed motion of a body in flight use analytic solutions to the equations of motion.¹⁻³ However, since both the equations of motion themselves and the aerodynamic coefficients that enter them are in general nonlinear, the analytic solutions involve various assumptions. Among the more common assumptions are small amplitudes of oscillation, linear aerodynamics, constant roll rate, constant freestream test conditions, constant model inertial properties, and axially symmetric models with only small asymmetries.

Auxiliary methods have been developed to remove some of these assumptions in special cases. For example, methods are available for determining a nonlinear static moment from the quasi-linear values of the moment obtained by analyzing a number of flights of a given configuration at different pitching amplitudes.^{3,4} Also, attempts have been made to effect analog integration of the equations of motion to match the observations. These latter efforts, while often useful, have lacked objectivity because they depend to some extent on individual judgment. No unique or "best" solution is possible.

It would be valuable to have a method of analysis free of the constraints mentioned. This paper describes such a method. First, the fundamentals used in applying the method are illustrated. Then the method is applied to four examples of varying complexity, and the diversity of its application is demonstrated. Alternate approaches for numerically fitting differential equations to experimental data, which lead to results equivalent to those obtained herein, are described in Refs. 5 and 6.

Method of Analysis

As in the case of existing methods, the basis of the present method is the minimization of the deviations of a set of ex-

perimental data from a calculated motion. The case in which only a single dependent variable α is involved will be considered first. We wish to minimize the sum of the squares of the residuals (SSR) defined as follows:

$$SSR = \sum_{i=1}^n [\alpha_{\text{exp}}(x_i) - \alpha_{\text{cal}}(x_i)]^2 \quad (1)$$

In the present context, α is the angle of attack, x_i is the distance measured along the flight path, and the subscripts exp and cal denote experimental and calculated values of the angle of attack. The summation extends over all n points at which data have been taken. Note that the independent variable x_i is assumed to be known exactly.

Traditionally in aeroballistic range work, an approximate closed-form solution for α and a conventional least-squares procedure are used to obtain all unknown constants in the solution. Should these constants appear in either a nonlinear or a transcendental manner, a least-squares technique employing differential corrections would be used. However, here we will assume that only an unsolved differential equation is at our disposal. For illustration, consider the following second-order nonlinear differential equation

$$\alpha'' + (C_1 + C_2\alpha^2)\alpha' + (C_3 + C_4\alpha^2)\alpha = 0 \quad (2)$$

with the initial conditions

$$\alpha(0) = C_5$$

$$\alpha'(0) = C_6$$

Primes denote derivatives with respect to distance x . The constants C_1 and C_2 define the nonlinear damping moment, and the constants C_3 and C_4 define the nonlinear static moment. We wish to determine the four aerodynamic parameters (C_1 - C_4) and the two initial conditions so that the sum of the squares of the residuals given by Eq. (1) is minimized. The method of differential corrections is used to do this.

A means to obtain initial values of the six unknowns required to start the differential correction procedure is outlined in the Appendix. Assume that we have these starting values, and expand α about this approximate solution using a Taylor

Presented as Paper 69-134 at the AIAA 7th Aerospace Sciences Meeting, New York, January 20-22, 1969; submitted February 3, 1969; revision received August 27, 1969.

* Research Scientist. Member AIAA.

† Research Scientist.

series. The result is

$$\alpha_{\text{cal}}(x_i) = \alpha_{\text{cal}}(x_i)_0 + \sum_{j=1}^6 \left(\frac{\partial \alpha}{\partial C_j} \right)_i \Delta C_j, i = 1, 2, \dots, n \quad (3)$$

where $\alpha_{\text{cal}}(x_i)_0$ is the value of α at x_i , obtained by numerical integration of Eq. (2) using the starting values for the six unknowns, and ΔC_j is the correction to the coefficient C_j to give a better fit. Substituting this equation into Eq. (1) yields

$$SSR = \sum_{i=1}^n \left[\alpha_{\text{exp}}(x_i) - \alpha_{\text{cal}}(x_i)_0 - \sum_{j=1}^6 \left(\frac{\partial \alpha}{\partial C_j} \right)_i \Delta C_j \right]^2 \quad (4)$$

If the partial derivatives in this equation were known, it would be a straightforward process to obtain the ΔC_j 's which, on an iterative basis, would minimize the SSR. Much time was spent by the authors in attempting to determine these partial derivatives with sufficient accuracy. An unsuccessful method will be described first to illustrate the problems.

The first attempt was to perturb, one at a time, the C_j 's, numerically integrate Eq. (2), and then form the partial derivatives using differences between the perturbed and unperturbed numerical solutions. This appeared to be a straightforward way of obtaining these derivatives. It did not lead to much success for the following reasons. If the perturbation chosen is too small, there will not be a big enough difference in the numerical solutions near the beginning of the integration to produce accurate derivatives. On the other hand, if the perturbation is large enough to get accurate derivatives near the start of the integration, the solution becomes so drastically different from the unperturbed solution at the end of the integration that the difference no longer represents a derivative. Using a fixed perturbation, the least-squares process diverged about half the time. Furthermore, when the least-squares process did converge, it converged to slightly different values depending on the size of the perturbation. It is very likely that this technique could be made to work with perturbations of many different sizes to get uniformly accurate results over a trajectory. However, a different approach was found to be the best solution.

The method that succeeded was that of parametric differentiation,⁷ which yields the partial derivatives with essentially uniform accuracy over the trajectory. It proceeds as follows. First define the following notation:

$$P_j = \frac{\partial \alpha}{\partial C_j}, P'_j = \frac{\partial P_j}{\partial x} = \frac{\partial \alpha'}{\partial C_j}, P''_j = \frac{\partial^2 P_j}{\partial x^2} = \frac{\partial \alpha''}{\partial C_j}$$

Note that it is explicitly assumed here that the order of differentiation can be reversed and that

$$\frac{\partial}{\partial C_j} \left(\frac{\partial \alpha}{\partial x} \right) = \frac{\partial}{\partial x} \left(\frac{\partial \alpha}{\partial C_j} \right)$$

For well-behaved functions, this is normally true.

Now differentiate Eq. (2) with respect to C_j to obtain the following six differential equations:

$$\begin{aligned} P''_1 + (C_1 + C_2 \alpha^2) P'_1 + (2C_2 \alpha \alpha' + C_3 + 3C_4 \alpha^2) P_1 &= -\alpha' \\ P''_2 + (C_1 + C_2 \alpha^2) P'_2 + (2C_2 \alpha \alpha' + C_3 + 3C_4 \alpha^2) P_2 &= -\alpha^2 \alpha' \\ P''_3 + (C_1 + C_2 \alpha^2) P'_3 + (2C_2 \alpha \alpha' + C_3 + 3C_4 \alpha^2) P_3 &= -\alpha \\ P''_4 + (C_1 + C_2 \alpha^2) P'_4 + (2C_2 \alpha \alpha' + C_3 + 3C_4 \alpha^2) P_4 &= -\alpha^3 \\ P''_5 + (C_1 + C_2 \alpha^2) P'_5 + (2C_2 \alpha \alpha' + C_3 + 3C_4 \alpha^2) P_5 &= 0 \\ P''_6 + (C_1 + C_2 \alpha^2) P'_6 + (2C_2 \alpha \alpha' + C_3 + 3C_4 \alpha^2) P_6 &= 0 \end{aligned} \quad (5)$$

The initial conditions for these equations are

$$\left. \begin{aligned} P_1 &= P_2 = P_3 = P_4 = P_5 = P_6 = 0 \\ P'_1 &= P'_2 = P'_3 = P'_4 = P'_5 = 0 \\ P_5 &= 1 \\ P'_6 &= 1 \end{aligned} \right\} \text{ at } x = 0 \quad (6)$$

Note that these are all linear differential equations with variable coefficients. However, both the variable coefficients and the right-hand sides of the first four equations are known from the numerical solution to Eq. (2). Numerical solutions to Eqs. (5) yield the partial derivatives of interest. The corrections (ΔC) to the six unknown coefficients can then be obtained by solving the matrix equation

$$[A] [\Delta C] = [B] \quad (7)$$

6 × 6 6 × 1 6 × 1

where general elements of the A and B matrices are given by

$$\begin{aligned} A_{jk} &= \sum_{i=1}^n \left(\frac{\partial \alpha}{\partial C_j} \right)_i \left(\frac{\partial \alpha}{\partial C_k} \right)_i \\ B_j &= \sum_{i=1}^n (\alpha_{\text{exp}} - \alpha_{\text{cal}})_i \left(\frac{\partial \alpha}{\partial C_j} \right)_i \end{aligned} \quad (8)$$

New values of the unknown coefficients C_j are obtained by adding ΔC_j to the present value, and the iteration process is continued until any prescribed degree of convergence is reached.

Application of the Method

As stated previously, the proposed method worked successfully only about 50% of the time until the method of parametric differentiation was incorporated to determine the required partial derivatives. Since this change, a converged solution has been obtained every time, despite the fact that more and more complicated differential equations have been used. Not enough experience is available, however, to set a limit on the complexity of the differential equations that can be treated or the number of unknown coefficients that can be determined from experimental data. To illustrate the validity and flexibility of the method, we will apply it to four different cases.

Linear Aerodynamics

The method was first applied to a case in which a solution is known, namely, the tri-cyclic solution of Ref. 1. Rather than deal with experimental data, exact trajectories were generated and used in testing the new approach. Explicitly assumed were linear aerodynamics and a constant roll rate (p). The differential equations involved are

$$\left. \begin{aligned} \alpha'' + A_1 \alpha' + A_2 \alpha - A_3 \sin p x + A_4 \cos p x + \frac{I_x}{I_y} p \beta' &= 0 \\ \beta'' + A_1 \beta' + A_2 \beta + A_3 \cos p x + A_4 \sin p x - \frac{I_x}{I_y} p \alpha' &= 0 \end{aligned} \right\} \quad (9)$$

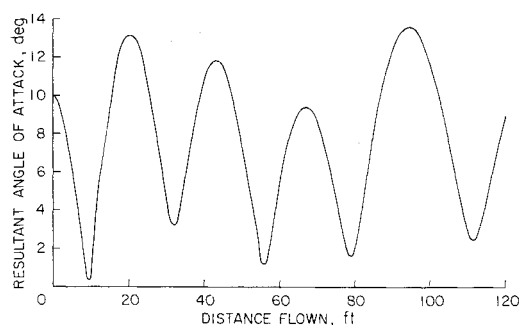
where α is the angle of attack and β is the angle of sideslip. Note that A_1 is related to the aerodynamic damping derivative, $C_{m\dot{\alpha}} + C_{m\dot{\alpha}}$, A_2 to the pitching-moment-curve slope, $C_{m\alpha}$ and A_3 and A_4 to the trim angle. A typical case analyzed is shown in Fig. 1; the resultant angle-of-attack is plotted vs distance flown in Fig. 1a, and a crossplot of α vs β is shown in Fig. 1b. Note in Fig. 1a that the distance between successive peaks is constant, characteristic of a linear system. The method reproduced exactly the nine

coefficients (p , A_1 to A_4 , four initial conditions) that generated the data, as it should. Most encouraging was the relatively short computer time needed to get a converged solution, and also the rate of convergence obtained. The computer time was essentially equivalent to that required for existing methods (≈ 1 min, IBM 7094). The rate of convergence was rapid. A sample of the rate of convergence, as given by the standard deviation of the fit from one iteration to the next, is as follows: 7.33° , 2.97° , 0.92° , 0.104° , 0.001° . The initial guesses of the coefficients were not critical; for the above example, every coefficient differed initially from its true value by at least 20%.

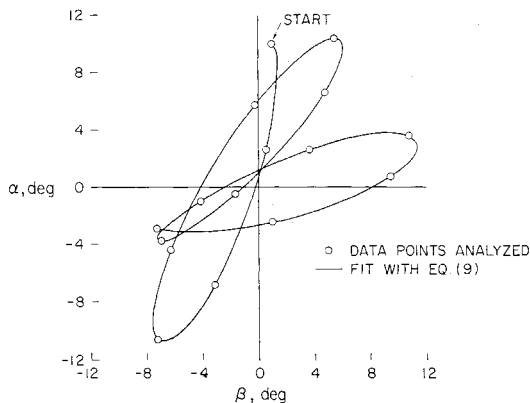
Nonlinear Aerodynamics

A series of ballistic-range tests of models of the Gemini capsule conducted about five years ago in the Ames Pressurized Ballistic Range indicated that both the static moment and the damping moment governing the model oscillations were nonlinear functions of angle of attack.⁸ Four of these flights were essentially planar and have been analyzed simultaneously[†] using the one-degree-of-freedom simulation given by Eq. (2). Twelve unknown coefficients were sought—four aerodynamic parameters and eight initial conditions, two for each flight. The solution converged as follows: $SD(\alpha) = 2.29^\circ$, 1.40° , 0.88° , 0.75° , 0.7426° , 0.7424° , and 0.7424° . The data points for the four flights together with the fit obtained by the new method are shown in Fig. 2. Values of the four coefficients C_1 through C_4 are as follows: $C_1 = -0.00607/\text{ft}$, $C_2 = 0.000105/\text{ft deg}^2$, $C_3 = 0.0208/\text{ft}^2$, $C_4 = -0.0000375/\text{ft}^2 \text{ deg}^2$.

Several points should be made at this time. The first is that the nonlinear static moment obtained by the present analysis is essentially the same as that obtained previously using the method of Ref. 4. This comparison is shown in Fig. 3. The authors were of the opinion that no previous



a) Resultant angle of attack vs distance.



b) α vs β .

Fig. 1 Motion involving linear aerodynamics.

[†] The nonlinearities were not strong enough to allow determination from a single flight with any precision.

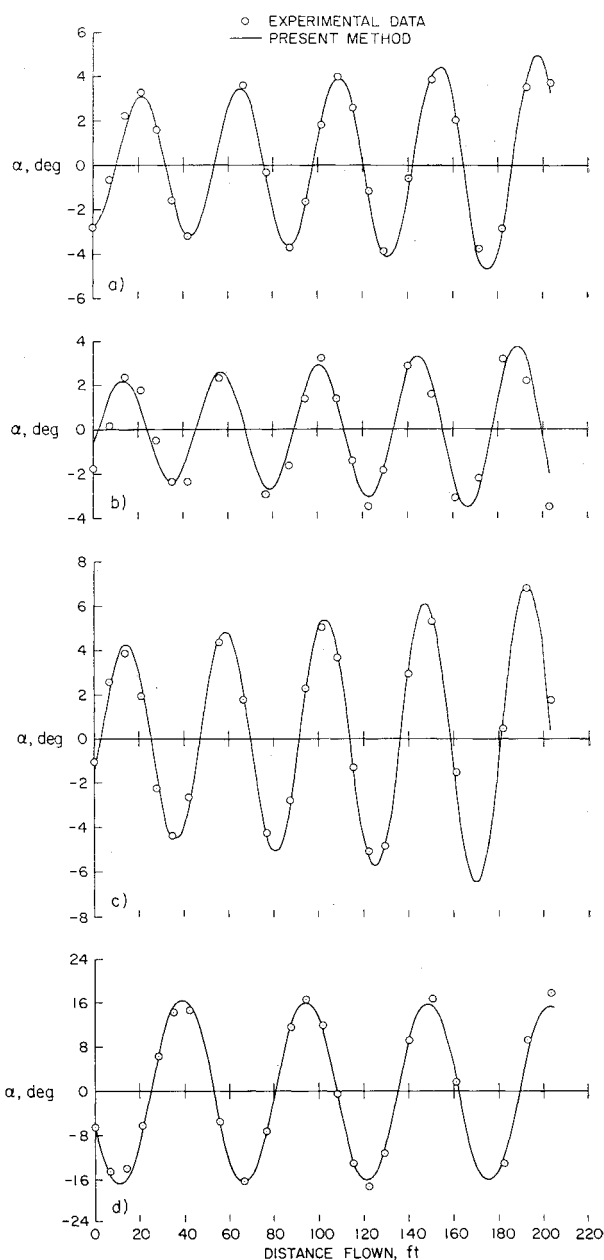


Fig. 2 Motions involving nonlinear aerodynamics; a) run 575; b) run 582; c) run 584; d) run 585.

techniques for obtaining the nonlinear damping moment from these data have been available. However this was proven incorrect by C. Murphy of BRL who, in private correspondence with the authors, successfully extracted the nonlinear damping moment using quasilinear techniques.³

Another point is that if one looks carefully at the fits to the experimental data shown in Fig. 2, three of the motions are matched very well, while run 582 leaves something to be desired. For this run (although small amplitude and hence small residuals), the fitted motion leads the data points at the early stations, reproduces the data well in the middle of the flight, and lags the data points at the end of the flight. When the present analysis was first performed, it was not realized that any intentional difference existed between the models tested in the four flights. However, the model tested in run 582 turned out to have had no "simulated window cutouts," whereas the models for the other three flights did. As discussed in Ref. 8, the effect of the window cutouts was relatively minor, but when more than one flight is being analyzed at once, as in the present case, minor differences in the aerodynamics can be detected. This kind of effect

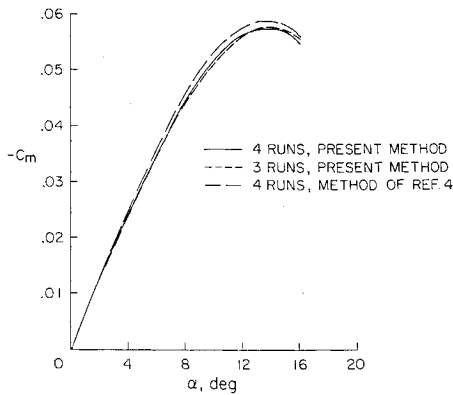


Fig. 3 Comparison of deduced moment coefficients.

becomes more pronounced with increasing distance flown. The three remaining runs, where the design model geometry was constant, were then analyzed together. As would be expected, the standard deviation in the fit did become better [$SD(\alpha) = 0.7183^\circ$], but the improvement was small due to the small amplitude of run 582. The values of C_1 – C_4 are now; $C_1 = -0.00549$, $C_2 = 0.000096$, $C_3 = 0.0204$, and $C_4 = -0.0000353$. These coefficients generate moments that differ only slightly from the previous set. The static moment obtained from these coefficients is also shown in Fig. 3.

Linear Aerodynamics, Variable Density

A frequent occurrence in countercurrent ballistic facilities is a variation in the air density along the model trajectory. Normally, the air density encountered by the model is known, and the variation is relatively small. In the past, an average air density of a particular flight (or portion of a flight) has been used to obtain the aerodynamic coefficients for that flight, even though the density was known to vary.

Since the present method can be adapted easily to permit varying air density, it was decided to compare this application with the previous solution which assumed an average density. The equations used were the same as Eq. (9), modified for an arbitrary density variation $\rho(x)$:

$$\left. \begin{aligned} \alpha'' + \rho(x)[B_1\alpha' + B_2\alpha - B_3\sin x + B_4\cos x] + \frac{I_x}{I_y} p\beta' &= 0 \\ \beta'' + \rho(x)[B_1\beta' + B_2\beta + B_3\cos x + B_4\sin x] - \frac{I_x}{I_y} p\alpha' &= 0 \end{aligned} \right\} \quad (10)$$

Again, exact trajectories were generated and then analyzed by the two methods. One density variation considered is shown in Fig. 4 and was presumed known exactly. Note that a variation this large would probably never be experienced in an actual ballistic-range test, but could be encountered in flights exiting (or entering) the atmosphere.

Figure 5 is analogous to Fig. 1 and shows the motion analyzed. Note in Fig. 5a that the distance between successive peaks is increasing with distance flown, due to the decreasing air density. A cross-plot of α vs β is shown in

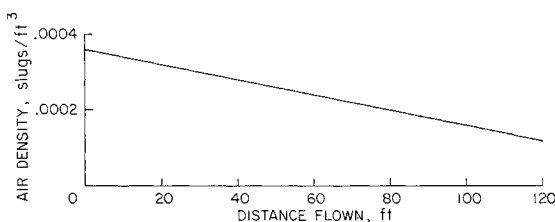


Fig. 4 Assumed density variation.

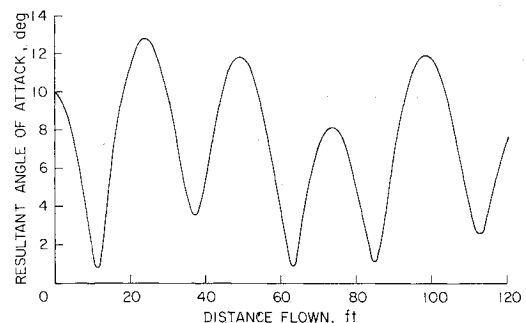
Fig. 5b. The present method converged identically to this solution. The rate of convergence is indicated as follows: $SD(\alpha^2 + \beta^2)^{1/2} = 4.99^\circ, 1.37^\circ, 0.13^\circ$, and 0.002° .

The fit obtained from the conventional "constant density" program² is shown in Fig. 6. As would be expected, some kind of "average" to the motion is obtained. Despite the large density variation assumed, this program still gives an excellent value for the moment-curve slope (-0.321 vs -0.316) and even a realistic measure of the aerodynamic damping (-6.37 after applying the corrections given in Ref. 3 vs -4.0). It should be emphasized, though, that it is risky to trust the deduced aerodynamics when any assumption is badly violated. Although useful results are often obtained, there is no guarantee of this being true in any particular case. An approach like the present method is preferable.

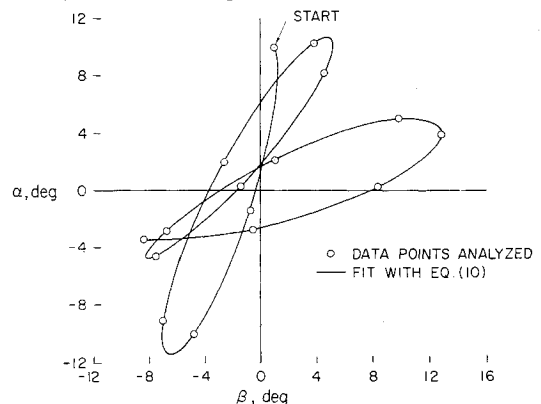
Large Amplitudes

A number of high-speed flights have been made of models of the Apollo Command Capsule in the Ames Hypervelocity Free-Flight Facility. These models were ballasted to move their center of gravity off the axis of symmetry, inducing a trim angle of roughly 30° . They were launched from a smooth-bore gun and the majority of the shots resulted in fairly planar motions having little roll. These shots could be successfully analyzed using existing data-reduction techniques and the major parameters of interest obtained (trim angle-of-attack, lift-curve slope, etc.).

Despite the lack of rifling in the gun, some of the models experienced high roll rates and hence motions were obtained that were anything but planar. Attempts were made to analyze these flights with existing data-reduction techniques, although it was realized that the results would be questionable because several assumptions were being violated (large amplitudes, large c.g. offset in conjunction with high roll rate). However, no results were obtained because the solutions diverged when these runs were analyzed. One such motion is shown in Fig. 7a where a crossplot of the Euler angles θ vs ψ is shown (yaw through ψ , pitch through θ , roll through ϕ). A hand fairing of the data is also indicated.



a) Resultant angle of attack vs distance.



b) α vs β .

Fig. 5 Motion involving varying air density.

The present method has been used on this particular flight with a number of different sets of differential equations. Convergence of the solution has been obtained in each instance. However, the standard deviation of the fit (in every case more than 3°) leaves much to be desired. A standard deviation this large means that the wrong differential equations are being used to analyze the motion. The major cause for not being able to determine the appropriate differential equations to use lies in the fact that the roll angle ϕ was not a measured parameter. Attempting to reconstruct the roll history in a complicated case such as this without any direct observations is difficult. Furthermore, with both large trim and roll rate, many aerodynamic derivatives normally neglected may be required to get a good fit.

The best fit obtained to the experimental data is shown in Fig. 7b. This fit was obtained assuming the roll rate to be a linear function of time (i.e., $p = p_0 + \dot{p}_0 t$). This representation resulted in a significantly better fit than that obtained assuming constant roll rate. Note that the basic character of the motion has been matched, although the standard deviation was 3.1° . Aerodynamic results from this fit gave a value of trim angle-of-attack that agreed closely with data from analysis of near-planar motions. The value of $C_m \alpha$ obtained also agreed closely with previous results. The fact that this flight could be analyzed at all is considered encouraging since the data previously had to be discarded as unusable. Note again that lack of a better fit to the motion is caused by not knowing the differential equations to use to match the motion (caused mainly by failure to measure roll orientation) rather than by any limitation inherent in the present method.

Concluding Remarks

A new approach to the problem of obtaining aerodynamic coefficients from an observed motion of a body in flight has been presented. More exact differential equations of motion can be considered by employing numerical techniques rather than approximate analytic solutions. The method of parametric differentiation allows the differential equations themselves to be used, by providing an accurate determination of the partial derivatives of the dependent variables with respect to the unknown coefficients. The examples presented show the new method to be very versatile. Not enough experience is yet available to know how complicated the governing differential equations can become and still be handled by the present approach.

Appendix: Starting Solution

In iterative solutions, the question arises as to how accurate the starting values of the coefficients must be to lead to convergence. If the starting solution does not roughly describe

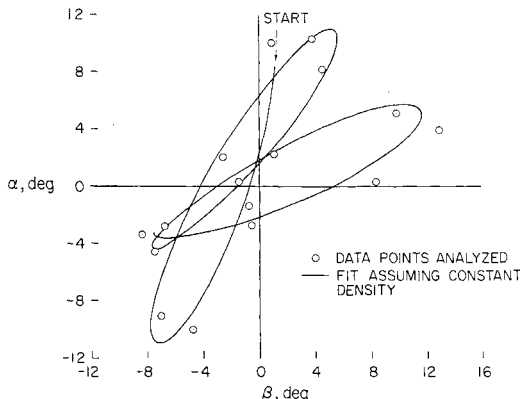
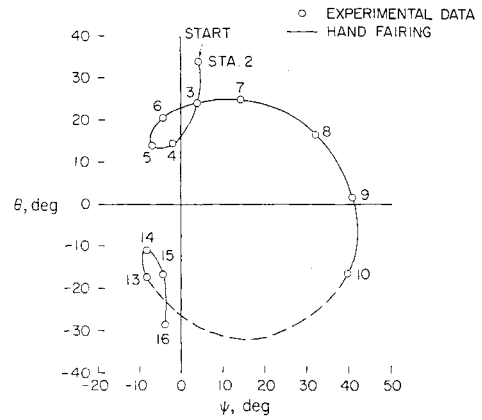
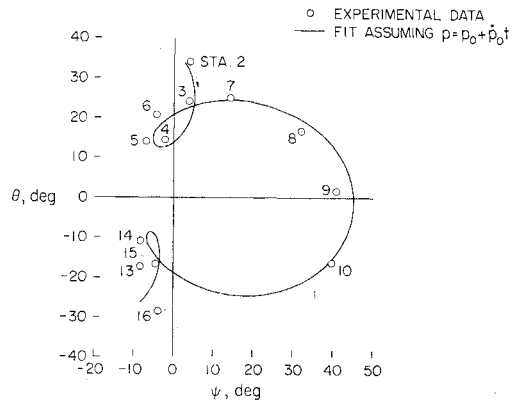


Fig. 6 Analysis of motion assuming constant density.



a) Hand fairing.



b) Computer solution.

Fig. 7 Motion involving a large trim angle.

the experimental data, divergence of the solution most often occurs. On the other hand, time spent in obtaining too accurate a solution may not be justified.

Consider the following differential equation [Eq. (2)]:

$$\alpha'' + (C_1 + C_2 \alpha^2) \alpha' + (C_3 + C_4 \alpha^2) \alpha = 0 \quad (A1)$$

with the initial conditions

$$\alpha(0) = \alpha_0 \quad \alpha'(0) = \alpha'_0$$

The coefficients C_1 - C_4 are not equally critical in determining an approximate fit to the data. In most cases, the critical coefficient is C_3 , which has the strongest effect on the frequency of the oscillatory motion. For nonlinearities that are not too large, C_1 , C_2 , and C_4 can be set initially to zero; a good guess of C_3 and the initial conditions, which can be obtained from hand-fairing the data, usually leads to convergence.

However, a procedure to give the starting solution more systematically and which also is not time consuming has been outlined in Ref. 9, and is as follows. Equation (A1) is integrated to yield

$$\alpha(x_i) = \alpha_0 + \left(\alpha'_0 + C_1 \alpha_0 + C_2 \frac{\alpha_0^3}{3} \right) x_i + C_1 \int_0^{x_i} \alpha dx + \frac{C_2}{3} \int_0^{x_i} \alpha^3 dx + C_3 \int_0^{x_i} \int_0^x \alpha dx dx + C_4 \int_0^{x_i} \int_0^x \alpha^3 dx dx \quad (A2)$$

If the data points are close enough together that reasonably good values of these integrals can be obtained, the method of least-squares can be used to obtain starting values of the coefficients and initial conditions. If the data are too sparse, this is not accurate since good integrations are not obtained. In such a case, the experimental data should be hand-faired and additional points from the fairing should be

used as data, but only in obtaining the starting values. Note that this method can give values of the coefficients that best fit any *given* fairing of the experimental data. To modify this fairing of the data and obtain a better fit requires the parametric differentiation technique described in this paper.

References

- ¹ Nicolaides, J. D., "On the Free-Flight Motion of Missiles Having Slight Configurational Asymmetries," BRL Rept. 858, AD 27405, 1953, Ballistic Research Labs., Aberdeen Proving Ground, Md.
- ² Malcolm, G. N. and Chapman, G. T., "A Computer Program for Systematically Analyzing Free-Flight Data to Determine the Aerodynamics of Axisymmetric Bodies," TN D-4766, 1968, NASA.
- ³ Murphy, C. H., "Free-Flight Motion of Symmetric Missiles," BRL Rept. 1216, AD 442757, 1963, Ballistic Research Labs., Aberdeen Proving Ground, Md.
- ⁴ Rasmussen, M. L. and Kirk, D. B., "On the Pitching and Yawing Motion of a Spinning Symmetric Missile Governed by an Arbitrary Nonlinear Restoring Moment," TN D-2135, 1964, NASA.
- ⁵ Bellman, R., Kagiwada, H., and Kalaba, R., "Quasilinearization, System Identification, and Prediction," RM-3812-PR, 1963, RAND Corp., Santa Monica, Calif.
- ⁶ Goodman, T. R., "System Identification and Prediction—An Algorithm Using a Newtonian Iteration Procedure," *Quarterly of Applied Mathematics*, Vol. XXIV, No. 3, Oct. 1966, pp. 249–255.
- ⁷ Rubbert, P. E. and Landahl, M. T., "Solution of the Transonic Airfoil Problem through Parametric Differentiation," *AIAA Journal*, Vol. 5, No. 3, March 1967, pp. 470–479.
- ⁸ Kruse, R. L., Malcolm, G. N., and Short, B. J., "Comparison of Free-Flight Measurements of Stability of the Gemini and Mercury Entry Capsules at Mach Numbers 3 and 9.5," TM X-957, 1964, NASA.
- ⁹ Boissevain, A. G. and Intrieri, P. F., "Determination of Stability Derivatives From Ballistic Range Tests of Rolling Aircraft Models," TM X-399, 1961, NASA.

APRIL 1970

AIAA JOURNAL

VOL. 8, NO. 4

A Transformation Theory for the Compressible Turbulent Boundary Layer with Mass Transfer

CONSTANTINO ECONOMOS*

General Applied Science Laboratories Inc., Westbury, N. Y.

The problem of the turbulent boundary layer with variable fluid properties and transpiration at constant pressure has been treated by modification and extension of the Coles' compressibility transformation. This analysis has been applied to several cases involving mass transfer both with and without chemical reactions. Comparison of these results with experiment has shown they yield more accurate predictions for gross boundary-layer properties than those obtained using earlier analyses. In addition, detailed analysis of velocity profiles has shown that the transformation correctly maps the "law of the wall" region to a constant property form. However, in complete analogy with the behavior observed by Baronti and Libby for the high-speed impermeable case, it is found that the transformation distorts the wake region of the profiles in the sense that the flat plate value of the Coles' wake parameter Π is not recovered. The magnitude of this distortion is shown to be roughly correlated by the density ratio ρ_w/ρ_e across the boundary layer.

Nomenclature

c_f, \bar{c}_f	= local skin-friction coefficients
F, \bar{F}	= $\rho_w v_w / \rho_e u_e, \bar{\rho} \bar{v}_w / \bar{\rho} \bar{u}_e$
k_1, k_2	= law of the wall constants, Eq. (21)
M	= Mach number
$R_x, R_{\bar{x}}$	= Reynolds numbers based on x, \bar{x}
$R_y, R_{\bar{y}}$	= Reynolds numbers based on y, \bar{y}
$R_\delta, R_{\bar{\delta}}$	= Reynolds numbers based on $\delta, \bar{\delta}$
$R_\theta, R_{\bar{\theta}}$	= Reynolds numbers based on $\theta, \bar{\theta}$
T, T_t	= temperature, total temperature

u, \bar{u}	= streamwise velocity components
\bar{U}	= $(2\bar{c}_f)^{1/2}[(1 + 2\bar{F}\bar{u}/\bar{c}_f)^{1/2} - 1]/\bar{F}$
v, \bar{v}	= normal velocity components
w	= functional form = $2\alpha^2(3 - 2\alpha)$
W	= molecular weight
x, \bar{x}	= streamwise coordinates
y, \bar{y}	= normal coordinates
Y	= mass fraction
α	= $R_{\bar{y}}/R_\delta$
$\delta, \bar{\delta}$	= boundary-layer thicknesses
$\zeta, \bar{\zeta}$	= $2F/c_f, 2\bar{F}/\bar{c}_f$
$\eta, \bar{\eta}, \sigma$	= parameters of the transformation
$\theta, \bar{\theta}$	= momentum thicknesses
$\mu, \bar{\mu}$	= coefficients of viscosity
Π	= Coles' wake parameter, Eq. (22)
$\rho, \bar{\rho}$	= densities
$\bar{\sigma}$	= $\sigma\mu_e/\bar{\mu}$
$\tau, \bar{\tau}$	= shear stresses (including Reynolds stresses)
Φ	= $\Phi = (\pi/k_1)(2 - w) - (1/k_1)\ln\alpha$
x, \bar{x}	= Reynolds numbers based on distance from arbitrary initial station
$\psi, \bar{\psi}$	= stream functions

Presented as Paper 69-161 at the AIAA 7th Aerospace Sciences Meeting, New York, January 20–22, 1969; submitted January 24, 1969; revision received August 21, 1969. Taken in part from the author's Ph.D. dissertation in the Polytechnic Institute of Brooklyn, Department of Aeronautics and Astronautics. This work was supported in part by NASA Contract NAS8-2686 and ARPA Contract DA-49-0830SA-3135. The author gratefully acknowledges the guidance and encouragement of P. Libby, University of California, San Diego.

* Supervisor, Thermochemistry and Viscous Flow Section. Member AIAA.